



www.ijbar.org

ISSN 2249-3352 (P) 2278-0505 (E)

Cosmos Impact Factor-5.86

Power Quality Enhancement Of Grid Tied Dual VSI Fed Microgrid With Fuzzy Based Controller

1 S. Bhavani Shankar, 2 N. Rupa Sri Prazna, 3 S. Srivani, 4 R. Haswitha, 5 Sk. Abdul Mateen, 6-B. Sarath Chandra

1,2,3,4,5, UG Students, Department of Electrical and Electronics Engineering

6, Asst. Professor, Department of Electrical and Electronics Engineering

RVR & JC College of Engineering, Chowdavaram, Guntur (Dt), AP, India.

Contact-bhavanishankar8985@gmail.com.

Abstract:

This paper presents a dual voltage source inverter (DVSI) scheme to enhance the power quality and reliability of a microgrid system. The proposed scheme consists of two inverters, allowing the microgrid to exchange power generated by distributed energy resources (DERs) while compensating for local unbalanced and nonlinear loads. A fuzzy logic controller (FLC) is employed instead of a PI controller to improve system performance, offering faster dynamic response, better adaptability, and reduced steady-state error. The control algorithms, based on instantaneous symmetrical component theory (ISCT), enable the DVSI to operate in grid-sharing and grid-injecting modes. The proposed scheme enhances system reliability, reduces the bandwidth requirement of the main inverter, lowers cost by minimizing the filter size, and ensures better utilization of microgrid power using a reduced dc-link voltage rating for the main inverter. These features make the DVSI scheme a promising option for microgrids supplying sensitive loads. The effectiveness of the proposed topology and control strategy is validated through extensive simulation and experimental results.

I. Introduction:

Technological progress and increasing environmental concerns are driving a paradigm shift in power systems, with greater integration of renewable energy sources through distributed generation (DG). These DG units, when coordinated with local generation and energy storage



systems, form a microgrid [1]. Within a microgrid, power from renewable sources such as fuel cells, photovoltaic (PV) systems, and wind energy systems is interfaced with the grid and local loads using power electronic converters. A grid-interactive inverter plays a vital role in exchanging power between the microgrid, the main grid, and connected loads [2], [3]. This inverter can function either in a grid-sharing mode, supplying a portion of the local load, or in a grid-injecting mode, delivering surplus power to the main grid.

Maintaining power quality is a critical requirement when a microgrid is connected to the utility grid. The widespread use of power electronic devices and nonlinear, unbalanced loads has contributed to a degradation in power quality within distribution networks. Additionally, feeder impedance in the distribution system can propagate harmonic currents, distorting the voltage at the point of common coupling (PCC). Meanwhile, industries with advanced automation—such as semiconductor manufacturing, chemical processing, and automotive production—demand high power quality, requiring effective compensation for nonlinear and unbalanced load currents [4].

Several studies have proposed the use of grid-interactive inverters in microgrids for both power injection and load compensation [5], [6]. A single inverter system with power quality enhancement capabilities is discussed in [7]. The focus of that work is on enabling dual functionalities within an inverter, including active power injection from a solar PV system and active power filtering for load compensation.

Voltage regulation and power flow control schemes using a wind energy system (WES) with distribution static compensators (DSTATCOMs) have been proposed for balancing power and stabilizing grid terminal voltages, even during wind fluctuations, using sliding mode control [8]. Other approaches involve multifunctional converters that simultaneously inject renewable power and compensate harmonics [9]. However, many of these solutions suffer from limitations when a single inverter is tasked with both injecting real power and compensating for load-related power quality issues. In such cases, the inverter's ability to perform load compensation is constrained by the real power availability from the microgrid [10]. For example, during peak solar insolation, the inverter's capacity to provide reactive power diminishes, although the demand for voltage regulation is highest during this time [11], [12].



To address this issue, this paper proposes a dual voltage source inverter (DVSI) scheme. In this configuration, the main voltage source inverter (MVSI) is dedicated to injecting real power from the microgrid, while an auxiliary voltage source inverter (AVSI) manages reactive power, harmonic compensation, and unbalanced load current compensation. This decoupling allows the MVSI to utilize its full capacity for real power transfer, assuming sufficient renewable energy is available at the DC link. Furthermore, splitting the load between two inverters reduces power losses across switching devices, enhances reliability, and allows the use of smaller, modular inverters operating at high switching frequencies—leading to reduced filter size and cost [13], [14].

To improve system adaptability and dynamic response under varying load and grid conditions, a fuzzy logic controller is integrated into the control scheme. Unlike traditional linear controllers, the fuzzy controller can handle system nonlinearities, parameter uncertainties, and imprecise inputs without requiring a precise mathematical model. It enhances control robustness, especially under conditions of a non-stiff grid and rapidly changing power demands.

The MVSI, responsible for real power injection, tracks only the fundamental positive sequence of current, which reduces its bandwidth requirement. Separate DC links are used for each inverter, allowing a three-phase three-leg topology with a single DC capacitor for the main inverter, further reducing DC link voltage requirements. Control algorithms are developed based on instantaneous symmetrical component theory (ISCT), with the fundamental PCC voltage sequence extracted using dq0 transformation [15], [16], [17]. The proposed fuzzy-based DVSI control strategy is validated through detailed simulation and experimental results in a three-phase four-wire distribution system, confirming its effectiveness in real-time grid-connected operation.

II. Proposed DVSI Topology

The proposed Dual Voltage Source Inverter (DVSI) topology is illustrated in Fig. 1. It comprises two inverters: an auxiliary voltage source inverter (AVSI) implemented using a Neutral Point Clamped (NPC) topology, and a main voltage source inverter (MVSI) configured as a conventional



three-leg inverter [18]. Both inverters are connected to the grid at the point of common coupling (PCC) and are responsible for supplying a nonlinear and unbalanced load.

In this setup, the AVSI is tasked with compensating for reactive power, harmonics, and unbalanced current components of the load. The three-phase load currents are denoted as i_{la} , i_{lb} , and i_{lc} , while i_{g_abc} , $i_{mu_gm_abc}$, and $i_{mu_gx_abc}$ represent the grid current, MVSI current, and AVSI current, respectively. The AVSI is powered by a split DC-link capacitor topology consisting of two capacitors, C1 and C2.

The MVSI serves to inject the available real power from the distributed energy resource (DER) into the grid. The DER can either be a DC source or an AC source connected through a rectifier. Renewable energy sources like fuel cells and photovoltaic (PV) systems typically produce low-voltage variable DC power, whereas variable-speed wind turbines generate variable-frequency AC power. Thus, a power conditioning stage is required before interfacing these sources with the MVSI. In this study, the DER is modeled as a DC source.

To mitigate high-frequency switching noise produced by the inverters, an inductor filter is employed at the inverter output [19]. Additionally, the distribution system is assumed to possess inherent feeder resistance (R_g) and inductance (L_g). These elements, combined with nonlinear loads, can cause harmonic distortion at the PCC voltage [20].

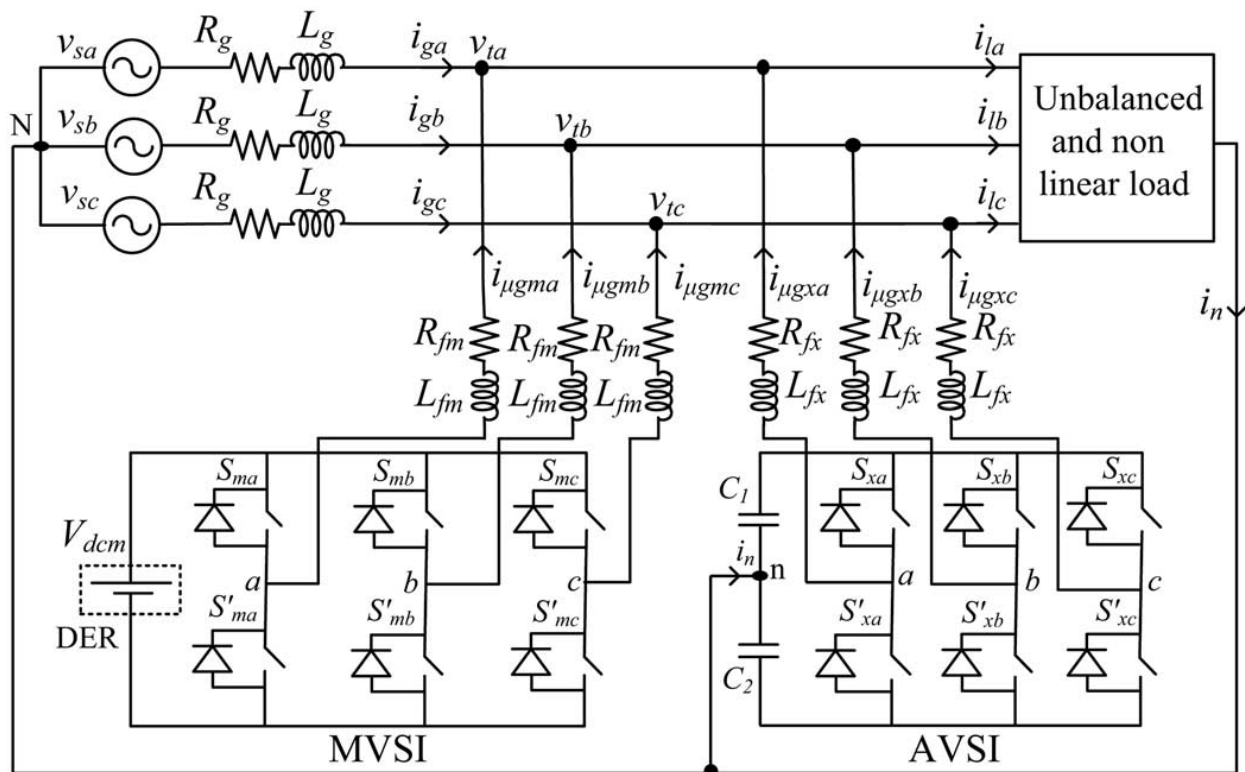


Fig. 1. Topology of proposed DVSI scheme.

A. Design of DVSI Parameters

1) Auxiliary Voltage Source Inverter (AVSI):

The critical parameters of the AVSI, including the DC-link voltage V_{dc} , DC-link capacitors $C1$ and $C2$, interfacing inductance L_{fx} , and hysteresis band pm_{hx} , are determined based on established design methods for split-capacitor DSTATCOM systems [16].

The DC-link voltage across each capacitor is chosen to be 1.6 times the peak of the phase voltage to ensure sufficient voltage margin. This results in a total DC-link voltage reference V_{dc_ref} of approximately 1040 V.

The sizing of the AVSI capacitors is based on the energy exchange that occurs during transient load changes. Suppose the total system load is rated at S kVA. In the worst-case scenario, the load can fluctuate between 0 and S , requiring the AVSI to temporarily supply or absorb real power to



stabilize system operation. This power exchange causes a temporary deviation in the capacitor voltage.

Assume the voltage controller takes n cycles i.e., nT seconds, where T is the system time period to respond during the transient. The maximum energy exchanged by the AVSI in this period is approximately nST . This energy must be stored or released by the DC-link capacitors, which leads to a voltage deviation. Therefore, the capacitance values are selected to limit the voltage variation during such transients, ensuring stability and reliability of compensation performance.

$$\frac{1}{2}C_1(V_{dcr}^2 - V_{dc1}^2) = nST$$

$$L_{fx} = \frac{1.6V_m}{4h_x f_{max}}$$

2) *MVSI*: The MVSI uses a three-leg inverter topology. Its dc-link voltage is obtained as $1.15*V_{ml}$, where V_{ml} is the peak value of line voltage. This is calculated to be 648 V. Also, MVSI supplies a balanced sinusoidal current at unity power factor. So, zero sequence switching harmonics will be absent in the output current of MVSI. This reduces the filter requirement for MVSI as compared to AVSI [21]. In this analysis, a filter inductance L_{fm} of 5 mH is used.

3). CONTROL STRATEGY FOR DVSI SCHEME

A. Fundamental Voltage Extraction

The control algorithm for reference current generation using ISCT requires balanced sinusoidal PCC voltages. Because of the presence of feeder impedance, PCC voltages are distorted. Therefore, the fundamental positive sequence components of the PCC voltages are extracted for the reference current generation.

To convert the distorted PCC voltages to balanced Fig. 2. Schematic diagram of PLL. sinusoidal voltages, $dq0$ transformation is used. The PCC voltages in natural reference frame (v_{ta} , v_{tb} , and v_{tc}) are first transformed into $dq0$ reference frame as given by



$$\begin{bmatrix} v_{td} \\ v_{tq} \\ v_{t0} \end{bmatrix} = C \begin{bmatrix} v_{ta} \\ v_{tb} \\ v_{tc} \end{bmatrix}$$

$$C = \sqrt{\frac{2}{3}} \begin{bmatrix} \sin \theta & \sin(\theta - \frac{2\pi}{3}) & \sin(\theta + \frac{2\pi}{3}) \\ \cos \theta & \cos(\theta - \frac{2\pi}{3}) & \cos(\theta + \frac{2\pi}{3}) \\ \frac{1}{\sqrt{2}} & \frac{1}{\sqrt{2}} & \frac{1}{\sqrt{2}} \end{bmatrix}.$$

In order to get θ , a modified synchronous reference frame (SRF) phase locked loop (PLL) [23] is used. The schematic diagram of this PLL is shown in Fig. 2. It mainly consists of a proportional integral (PI) controller and an integrator. In this PLL, the SRF terminal voltage in q -axis (v_{tq}) is compared with 0 V and the error voltage thus obtained is given to the PI controller. The frequency deviation $\Delta\omega$ is then added to the reference frequency ω_0 and finally given to the integrator to get θ . It can be proved that, when, $\theta = \omega_0 t$ and by using the Park's transformation matrix (C), q -axis voltage in $dq0$ frame becomes zero and hence the PLL will be locked to the reference frequency (ω_0). As PCC voltages are distorted, the transformed voltages in $dq0$ frame (v_{td} and v_{tq}) contain average and oscillating components of voltages. These can be represented as

$$v_{td} = \bar{v}_{td} + \tilde{v}_{td}, \quad v_{tq} = \bar{v}_{tq} + \tilde{v}_{tq}$$

where v_{td} and v_{tq} represent the average components of v_{td} and v_{tq} , respectively. The terms $_v_{td}$ and $_v_{tq}$ indicate the oscillating components of v_{td} and v_{tq} , respectively. Now the fundamental positive sequence of PCC voltages in natural reference frame can be obtained with the help of inverse $dq0$ transformation as given by

$$\begin{bmatrix} v_{ta1}^+ \\ v_{tb1}^+ \\ v_{tc1}^+ \end{bmatrix} = C^T \begin{bmatrix} \bar{v}_{td} \\ \bar{v}_{tq} \\ 0 \end{bmatrix}.$$

B. Instantaneous Symmetrical Component Theory



ISCT was developed primarily for unbalanced and nonlinear load compensations by active power filters. The system topology shown in Fig. 2 is used for realizing the reference current for the compensator [15]. The ISCT for load compensation is derived based on the following three conditions.

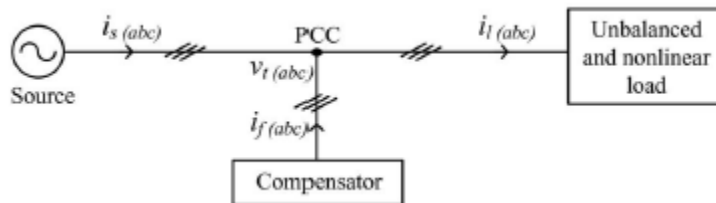


Fig. 2. Schematic of an unbalanced and nonlinear load compensation scheme.

C. Control Strategy of DVSI

Control strategy of DVSI is developed in such a way that grid and MVSI together share the active load power, and AVSI supplies rest of the power components demanded by the load.

1) Reference Current Generation for Auxiliary Inverter:

The dc-link voltage of the AVSI should be maintained constant for proper operation of the auxiliary inverter. DC-link voltage variation occurs in auxiliary inverter due to its switching and ohmic losses. These losses termed as P_{loss} should also be supplied by the grid. An expression for P_{loss} is derived on the condition that average dc capacitor current is zero to maintain a constant capacitor voltage [15]. The deviation of average capacitor current from zero will reflect as a change in capacitor voltage from a steady state value.

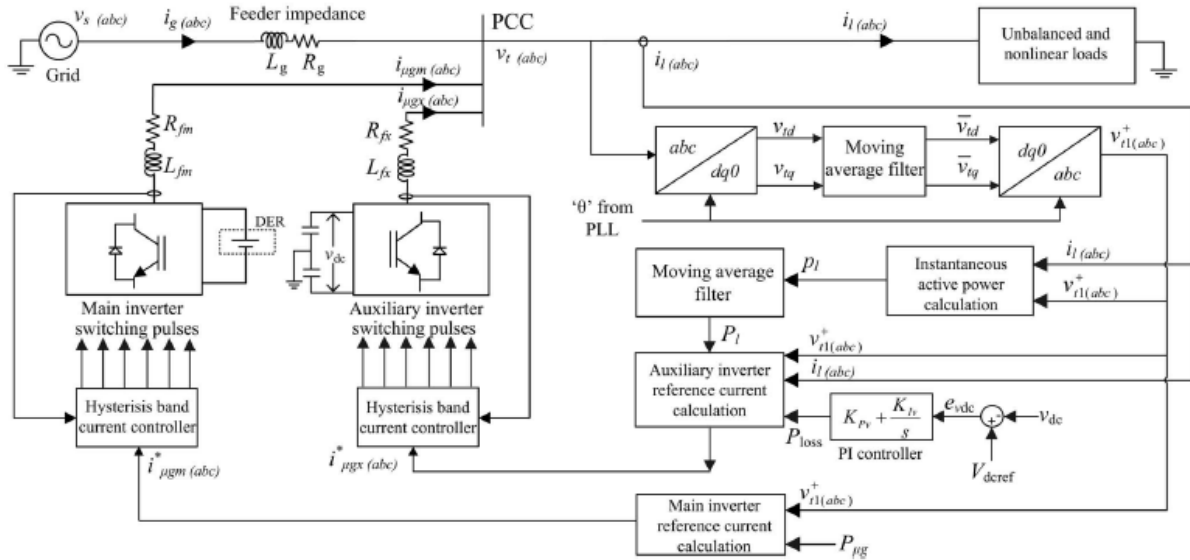


Fig. 3. Schematic diagram showing the control strategy of proposed DVSI scheme.

$$P_{\text{loss}} = K_{Pv} e_{vdc} + K_{Iv} \int e_{vdc} dt$$

where $e_{vdc} = V_{dcref} - v_{dc}$, v_{dc} represents the actual voltage sensed and updated once in a cycle. In the above equation, K_{Pv} and K_{Iv} represent the proportional and integral gains of dc-link PI controller, respectively. The P_{loss} term thus obtained should be supplied by the grid, and therefore AVSI reference currents can be obtained as given in (14). Here, the dc-link voltage PI controller gains are selected so as to ensure stability and better dynamic response during load change [24]

$$i_{\mu g x a}^* = i_{l a} - \left(\frac{v_{t a 1}^+}{\sum_{j=a,b,c} v_{t j}^+} \right) (P_l + P_{\text{loss}})$$

$$i_{\mu g x b}^* = i_{l b} - \left(\frac{v_{t b 1}^+}{\sum_{j=a,b,c} v_{t j}^+} \right) (P_l + P_{\text{loss}})$$

$$i_{\mu g x c}^* = i_{l c} - \left(\frac{v_{t c 1}^+}{\sum_{j=a,b,c} v_{t j}^+} \right) (P_l + P_{\text{loss}}).$$



2) Reference Current Generation for Main Inverter:

MVSI supplies balanced sinusoidal currents based on the available renewable power at DER. If MVSI losses are neglected, the power injected to grid will be equal to that available at DER ($P_{\mu g}$). The following equation, which is derived from ISCT can be used to generate MVSI reference currents for three phases ($a, b,$ and c)

$$i_{\mu gm(abc)}^* = \left(\frac{v_{t(abc)1}^+}{\sum_{j=a,b,c} v_{tj}^+{}^2} \right) P_{\mu g}$$

where $P_{\mu g}$ is the available power at the dc link of MVSI.

The reference currents obtained from (14) to (15) are tracked by using hysteresis band current controller (HBCC). HBCC schemes are based on a feedback loop, usually with a two-level

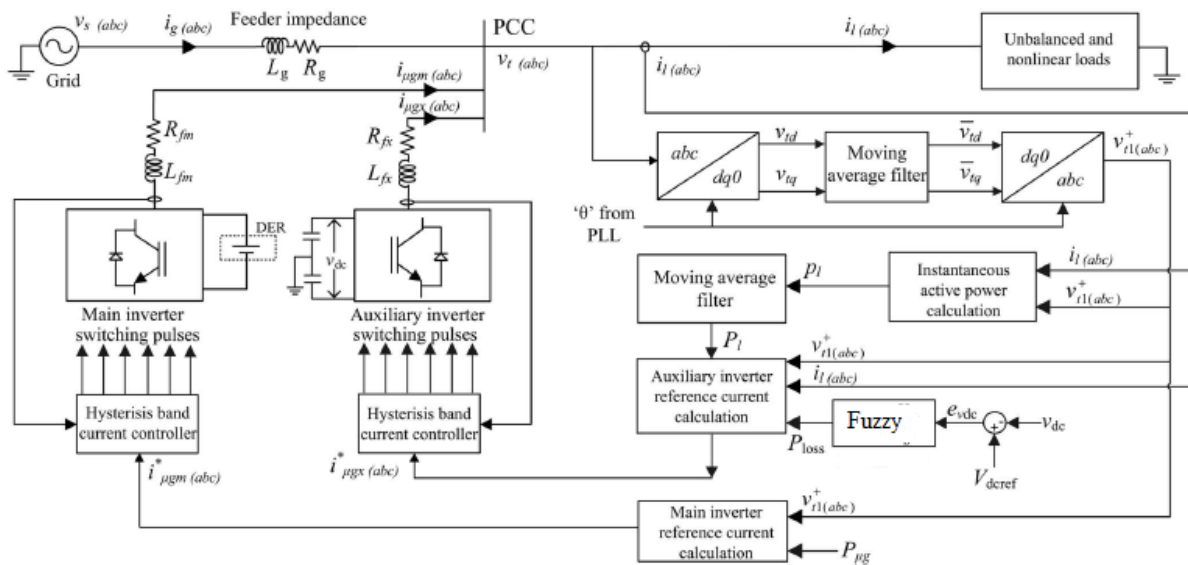


Fig. 4. Schematic diagram showing the control strategy of proposed DVSI scheme.

comparator. This controller has the advantage of peak current limiting capacity, good dynamic response, and simplicity in implementation [14]. A hysteresis controller is a high-gain proportional controller. This controller adds certain phase lag in the operation based on the hysteresis band and will not make the system unstable. Also, the proposed DVSI scheme uses a



first-order inductor filter which retains the closed-loop system stability [25]. The entire control strategy is schematically represented in Fig. 4. Applying Kirchoff’s current law (KCL) at the PCC in Fig. 4

Parameters	Values
Grid voltage	400 V(L-L)
Fundamental frequency	50 Hz
Feeder impedance	$R_g = 0.5 \Omega, L_g = 1.0 \text{ mH}$
AVSI	$C_1 = C_2 = 2000 \mu\text{F}$ $V_{dcref} = 1040 \text{ V}$ Interfacing inductor, $L_{fx} = 20 \text{ mH}$ Inductor resistance, $R_{fx} = 0.25 \Omega$ Hysteresis band ($\pm h_x$) = 0.1 A
MVSI	DC-link voltage, $V_{dcM} = 650 \text{ V}$ Interfacing inductor, $L_{fm} = 5 \text{ mH}$ Inductor resistance, $R_{fm} = 0.25 \Omega$ Hysteresis band ($\pm h_m$) = 0.1 A
Unbalanced linear load	$Z_{la} = 35 + j19 \Omega$ $Z_{lb} = 30 + j15 \Omega$ $Z_{lc} = 23 + j12 \Omega$
Nonlinear load	3 ϕ diode bridge rectifier with DC side current of 3.0 A
DC voltage controller gains	$K_{pv} = 10, K_{fv} = 0.05$

TABLE 1 – SYSTEM PARAMETERS FOR SIMULATIONSTUDY

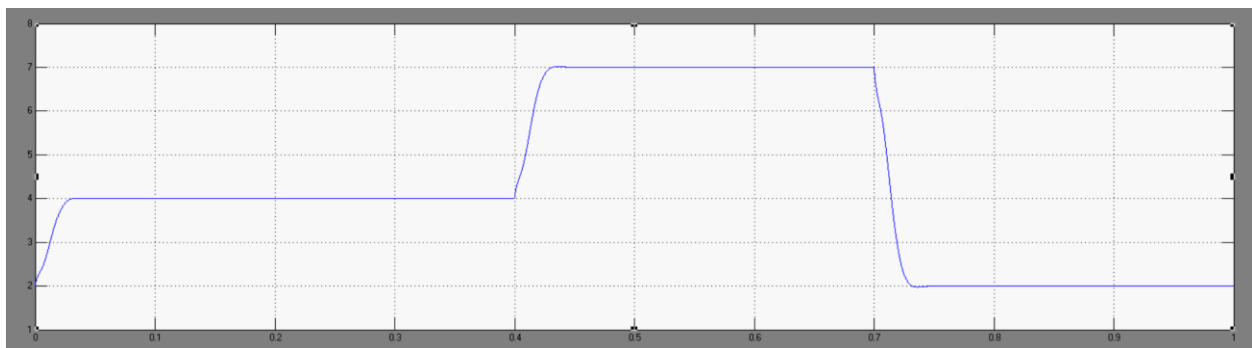
SIMULATION STUDIES:



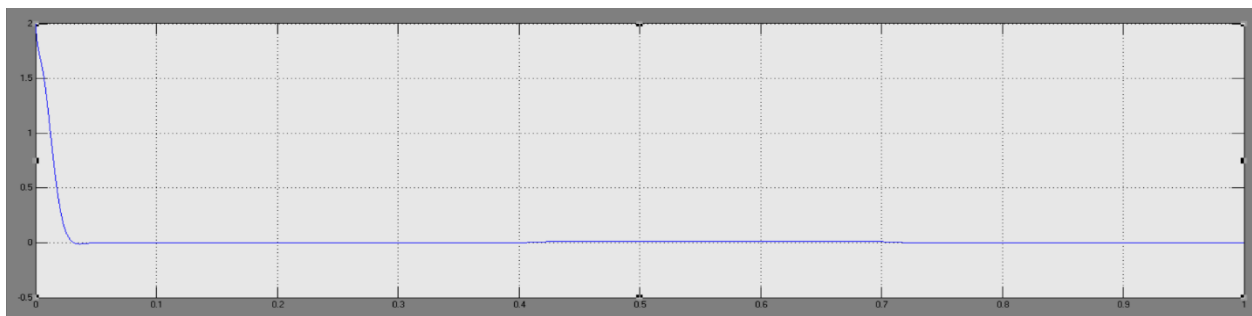
5(a). Load active power



5(b). Active power supplied by grid

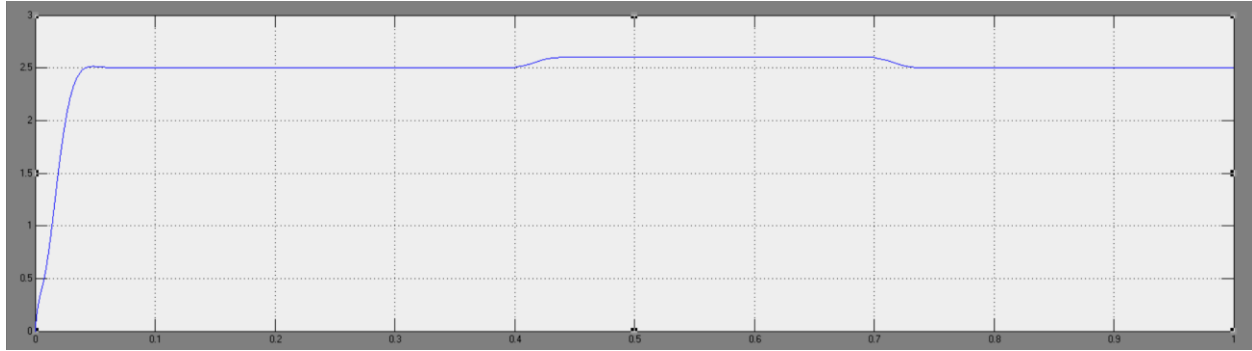


5(c). Active power supplied by MVSI

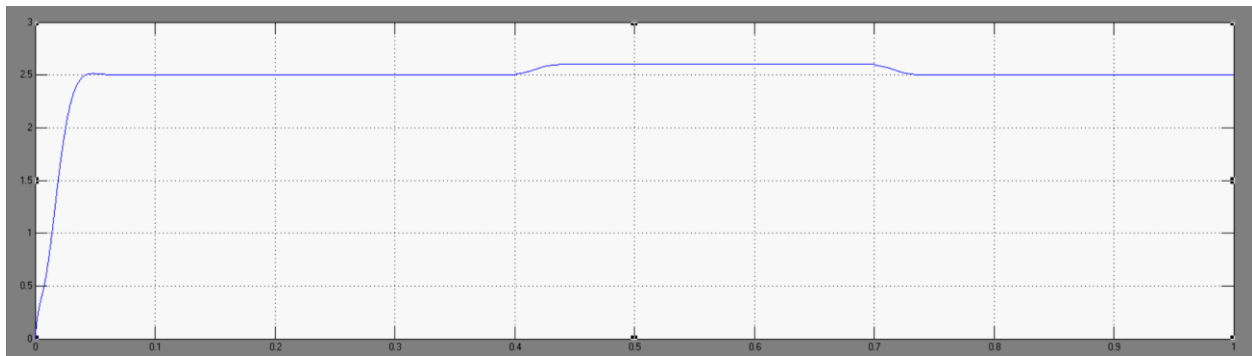


5(d). Active power supplied by AVSI:

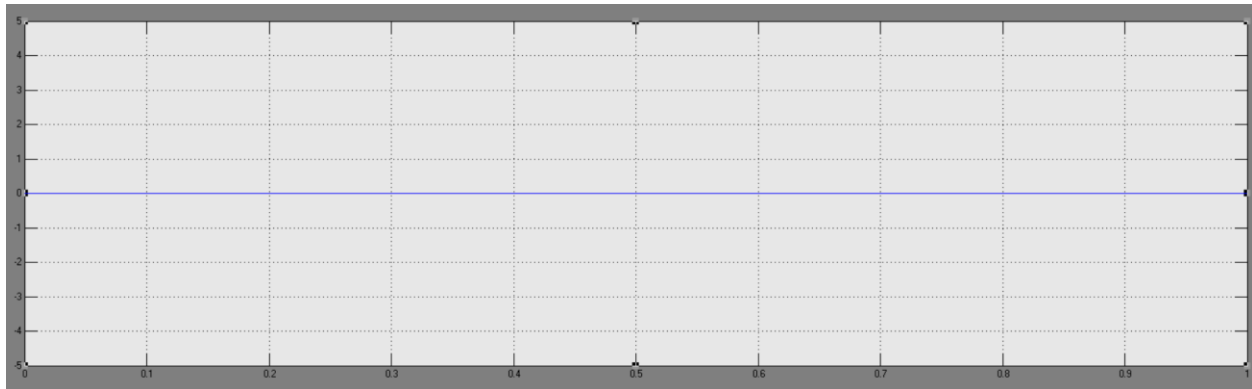
Fig 5-Active power sharing



6(a). load reactive power

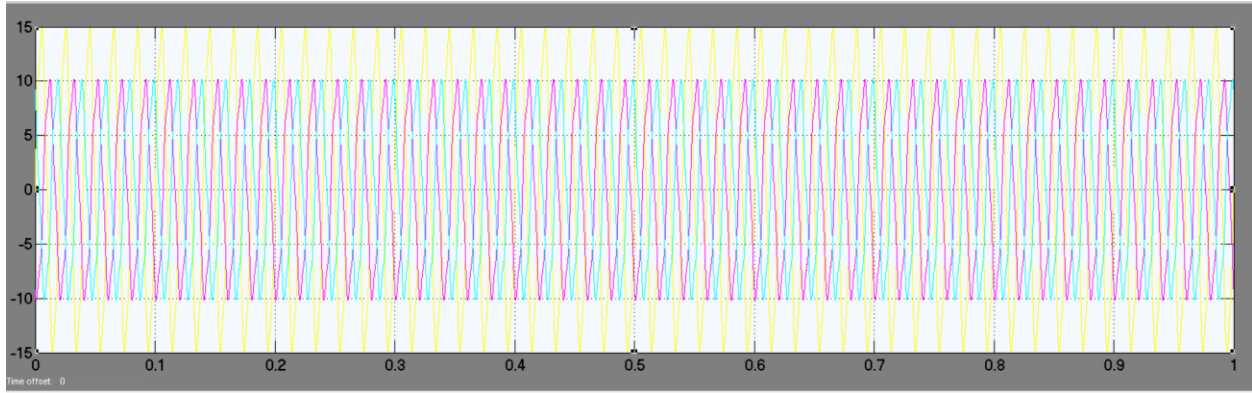


6(b). Reactive power supplied by AVSI.

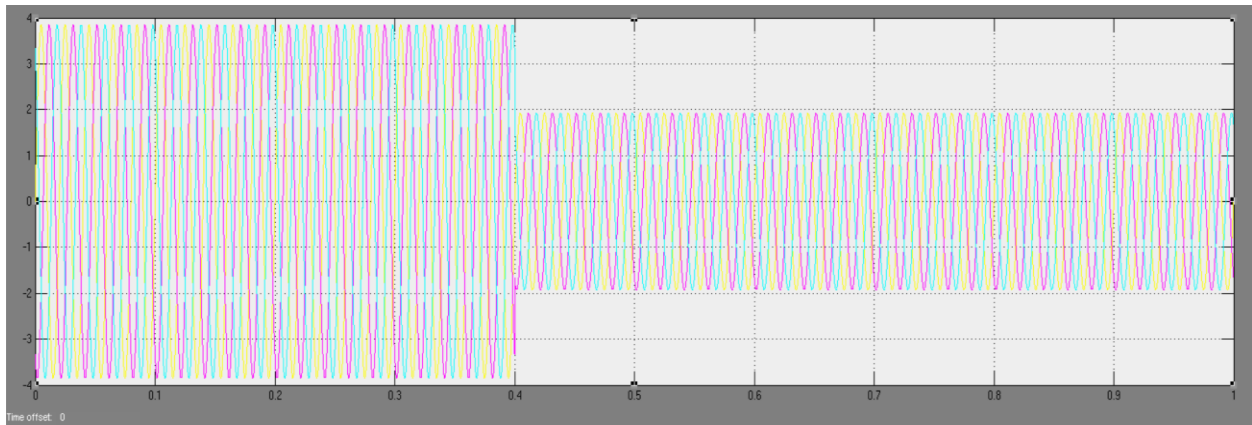


6(c). Reactive power supplied by MVSI.

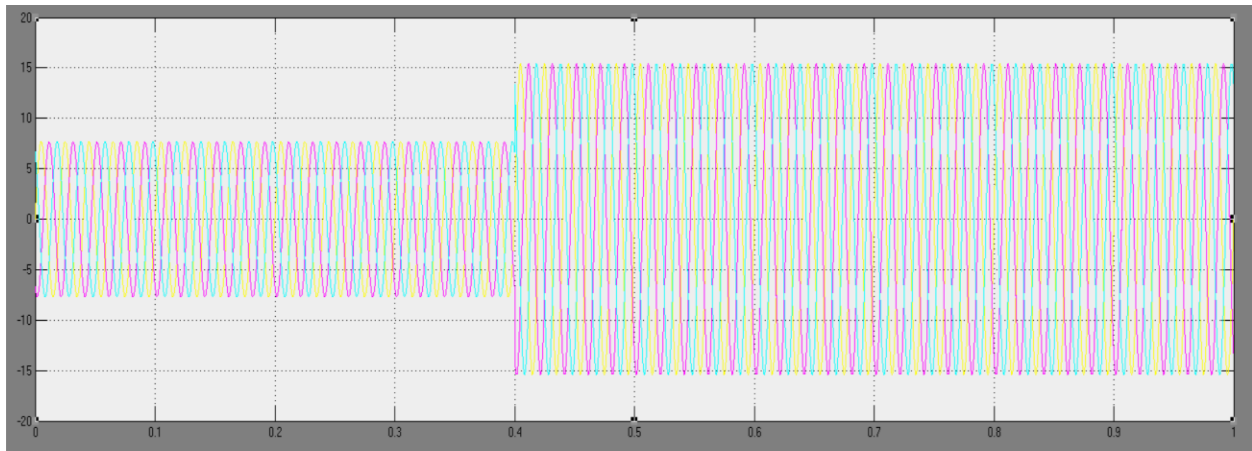
Fig 6: Reactive power sharing



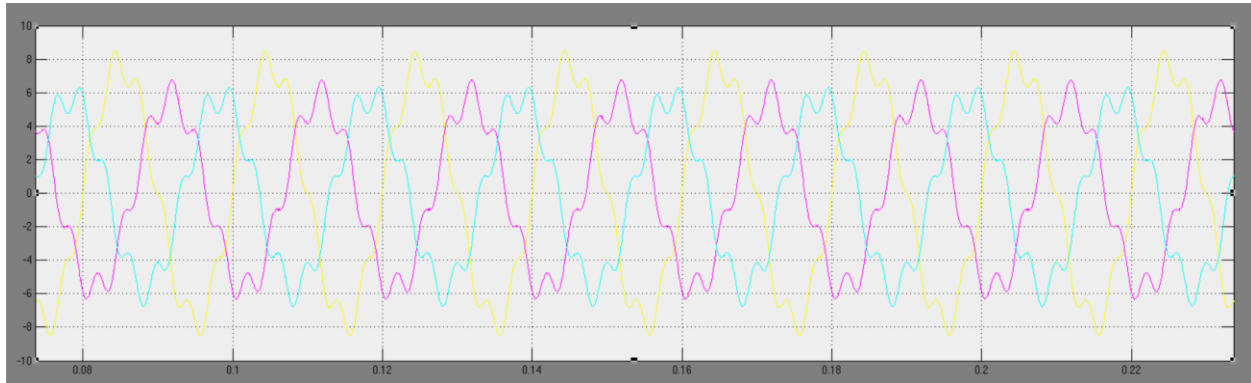
7(a). Load currents



7(b). Grid currents



7(c). MVSI Currents



7(d). AVSI currents.

Fig7: Simulated performance of DVSI Scheme

The simulation model of the proposed DVSI scheme, as illustrated in Fig. 1, has been developed using PSCAD 4.2.1 to evaluate its performance under both steady-state and transient operating conditions. The system parameters used for the simulation are provided in Table I.

This simulation study highlights the capability of the DVSI system to operate in grid sharing as well as grid injecting modes. The voltage distortion at the Point of Common Coupling (PCC) due to feeder impedance in the absence of DVSI. These distorted voltages, if directly used for reference current generation of the AVSI, would lead to ineffective compensation [14].

To address this, the fundamental positive sequence of PCC voltages is extracted using the algorithm described in Section III-A. These purified voltages are then used to generate accurate reference currents for both MVSIs and AVSI.

1). The performance of the DVSI scheme in terms of active power distribution is shown in Fig. 5(a)–(d), which depicts:

- Load active power demand (P_l),
- Grid-supplied active power (P_g),
- Active power delivered by MVSIs ($P_{\mu g}$),
- Active power contribution from AVSI (P_x).



From $t = 0.1$ s to 0.4 s, MVSI supplies 4 kW while the load demand is 6 kW, so the remaining 2 kW is drawn from the grid—indicating grid sharing operation. At $t = 0.4$ s, the microgrid output increases to 7 kW, exceeding the load demand. This triggers a transition to grid injecting mode, and the excess 1 kW is fed into the grid, reflected as negative grid power in the plot.

2). Reactive power dynamics are shown in Fig. 6(a)–(c):

- Load reactive power (Q_l),
- Reactive power from AVSI (Q_x),
- Reactive power from MVSI ($Q_{\mu g}$).

The results confirm that AVSI solely compensates for the entire load reactive power, as intended by design.

3). Waveforms for different currents are presented in Fig. 7(a)–(d), including:

- Load currents ($i_l(abc)$),
- Grid currents ($i_g(abc)$),
- MVSI currents ($i_{\mu g}(abc)$),
- AVSI currents ($i_{\mu x}(abc)$).

The load currents are both unbalanced and distorted, while the MVSI and grid currents remain balanced and sinusoidal, demonstrating the AVSI's effectiveness in compensating harmonics and unbalances.

These simulation results comprehensively validate the effectiveness of the DVSI system with a fuzzy controller, demonstrating its capability for:

- Accurate load compensation (reactive, harmonic, and unbalanced currents),
- Efficient active power injection from DG units,



- High power quality,
- And robust performance under dynamic grid conditions in a microgrid environment.

III. Conclusion

This paper has presented a Dual Voltage Source Inverter (DVSI) scheme integrated with a Fuzzy Logic Controller (FLC) to enhance the performance and reliability of microgrid systems. By separating the functions of power injection and load compensation between two dedicated inverters, the DVSI topology ensures optimal utilization of Distributed Energy Resources (DERs) while maintaining high power quality under varying load and grid conditions. The use of a FLC in place of a conventional PI controller significantly improves dynamic response, adaptability to system variations, and reduces steady-state errors, making the control strategy more robust.

The control algorithms, developed using Instantaneous Symmetrical Component Theory (ISCT), enable seamless operation in both grid-sharing and grid-injecting modes, ensuring stable operation across different scenarios. Additionally, the proposed scheme demonstrates several advantages including improved system flexibility, reduced filter size and cost, lower dc-link voltage requirements, and enhanced reliability.

Extensive simulation and experimental validation confirm the effectiveness of the DVSI scheme in providing clean and reliable power to sensitive loads in a microgrid environment. Overall, the proposed system offers a viable and efficient solution for future smart grid and renewable energy integration applications.

REFERENCES:

- [1] A. Kahrobaeian and Y.-R. Mohamed, "Interactive distributed generation interface for flexible micro-grid operation in smart distribution systems," *IEEE Trans. Sustain. Energy*, vol.3, no. 2, pp. 295–305, Apr. 2012.
- [2] N. R. Tummuru, M. K. Mishra, and S. Srinivas, "Multifunctional VSC controlled microgrid using instantaneous symmetrical components theory," *IEEE Trans. Sustain. Energy*, vol. 5, no.1, pp. 313–322, Jan. 2014.



- [3] Y. Zhang, N. Gatsis, and G. Giannakis, “Robust energy management for microgrids with high-penetration renewables,” *IEEE Trans. Sustain. Energy*, vol. 4, no. 4, pp. 944–953, Oct.2013.
- [4] R. Majumder, A. Ghosh, G. Ledwich, and F. Zare, “Load sharing and power quality enhanced operation of a distributed microgrid,” *IET Renewable Power Gener.*, vol. 3, no. 2, pp. 109–119, Jun. 2009.
- [5] J. Guerrero, P. C. Loh, T.-L. Lee, and M. Chandorkar, “Advanced control architectures for intelligent microgrids—Part II: Power quality, energy storage, and ac/dc microgrids,” *IEEE Trans. Ind. Electron.*, vol. 60, no. 4, pp. 1263–1270, Dec. 2013.
- [6] Y. Li, D. Vilathgamuwa, and P. C. Loh, “Microgrid power quality enhancement using a three-phase four-wire grid-interfacing compensator,” *IEEE Trans. Ind. Appl.*, vol. 41, no. 6, pp. 1707–1719, Nov. 2005.
- [7] M. Schonardie, R. Coelho, R. Schweitzer, and D. Martins, “Control of the active and reactive power using dq0 transformation in a three-phase grid-connected PV system,” in *Proc. IEEE Int. Symp. Ind. Electron.*, May 2012, pp. 264–269.
- [8] R. S. Bajpai and R. Gupta, “Voltage and power flow control of grid connected wind generation system using DSTATCOM,” in *Proc. IEEE Power Energy Soc. Gen. Meeting—Convers. Del. Elect. Energy 21st Century*, Jul. 2008, pp. 1–6.
- [9] M. Singh, V. Khadkikar, A. Chandra, and R. Varma, “Grid interconnection of renewable energy sources at the distribution level with power-quality improvement features,” *IEEE Trans. Power Del.*, vol. 26, no. 1, pp. 307–315, Jan. 2011.
- [10] H.-G. Yeh, D. Gayme, and S. Low, “Adaptive VAR control for distribution circuits with photovoltaic generators,” *IEEE Trans. Power Syst.*, vol. 27, no. 3, pp. 1656–1663, Aug. 2012.
- [11] C. Demoulias, “A new simple analytical method for calculating the optimum inverter size in grid-connected PV plants,” *Electr. Power Syst. Res.*, vol. 80, no. 10, pp. 1197–1204, 2010.



- [12] R. Tonkoski, D. Turcotte, and T. H. M. EL-Fouly, “Impact of high PV penetration on voltage profiles in residential neighborhoods,” *IEEE Trans. Sustain. Energy*, vol. 3, no. 3, pp. 518–527, Jul. 2012.
- [13] X. Yu and A. Khambadkone, “Reliability analysis and cost optimization of parallel-inverter system,” *IEEE Trans. Ind. Electron.*, vol. 59, no. 10, pp. 3881–3889, Oct. 2012.
- [14] M. K. Mishra and K. Karthikeyan, “Design and analysis of voltage source inverter for active compensators to compensate unbalanced and nonlinear loads,” in *Proc. IEEE Int. Power Eng. Conf.*, 2007, pp. 649–654.
- [15] A. Ghosh and A. Joshi, “A new approach to load balancing and power factor correction in power distribution system,” *IEEE Trans. Power Del.*, vol. 15, no. 1, pp. 417–422, Jan. 2000.
- [16] U. Rao, M. K. Mishra, and A. Ghosh, “Control strategies for load compensation using instantaneous symmetrical component theory under different supply voltages,” *IEEE Trans. Power Del.*, vol. 23, no. 4, pp. 2310–2317, Oct. 2008.
- [17] P. Rodriguez *et al.*, “A stationary reference frame grid synchronization system for three-phase grid-connected power converters under adverse grid conditions,” *IEEE Trans. Power Electron.*, vol. 27, no. 1, pp. 99–112, Jan. 2012.
- [18] S. Iyer, A. Ghosh, and A. Joshi, “Inverter topologies for DSTATCOM applications—A simulation study,” *Electr. Power Syst. Res.*, vol. 75, no. 23, pp. 161–170, 2005.
- [19] Y. Tang, P. C. Loh, P. Wang, F. H. Choo, and F. Gao, “Exploring inherent damping characteristic of LCL filters for three-phase grid-connected voltage source inverters,” *IEEE Trans. Power Electron.*, vol. 27, no. 3, pp. 1433–1443, Mar. 2012.
- [20] D. Vilathgamuwa, P. C. Loh, and Y. Li, “Protection of microgrids during utility voltage sags,” *IEEE Trans. Ind. Electron.*, vol. 53, no. 5, pp. 1427–1436, Oct. 2006.



- [21] M. Prodanovic and T. Green, "Control and filter design of three-phase inverters for high power quality grid connection," *IEEE Trans. Power Electron.*, vol. 18, no. 1, pp. 373–380, Jan.2003.
- [22] M. Hamid, A. Jusoh, and M. Anwari, "Photovoltaic plant with reduced output current harmonics using generation-side active power conditioner," *IET Renewable Power Gener.*, vol. 8, no. 7, pp. 817–826, Sep.2014.
- [23] L. Rolim, D. da Costa, and M. Aredes, "Analysis and software implementation of a robust synchronizing PLL circuit based on the pq theory," *IEEE Trans. Ind. Electron.*, vol. 53, no. 6, pp. 1919–1926, Dec. 2006.
- [24] L. Shiguo, "Optimal design of dc voltage close loop control for an active power filter," in *Proc. IEEE Int. Conf. Power Electron. Drive Syst.*, Feb. 1995, pp. 565–570.
- [25] A. Ghosh and G. Ledwich, "Load compensating DSTATCOM in weak AC systems," *IEEE Trans. Power Del.*, vol. 18, no. 4, pp. 1302–1309, Oct. 2003.